10 Orbitals, Frustration and Quantum Criticality

Matthias Vojta
Institut für Theoretische Physik
Technische Universität Dresden

Contents

E. Pavarini and E. Koch (eds.)
Orbital Physics in Correlated Matter
Modeling and Simulation Vol. 13
Forschungszentrum Jülich, 2023, ISBN 978-3-95806-689-2
http://www.cond-mat.de/events/correl23

1 Introduction

This chapter is devoted to phase transitions at zero temperature, usually called quantum phase transitions (QPT), their critical behavior, and its changes arising from frustration and the presence of orbital degrees of freedom [1].

QPT and quantum criticality define an active field of research which goes back to the work of Hertz in 1976 [2] who considered magnetic ordering transitions in metals. Much progress was made in the 1990s and 2000s [3], such that many classes of symmetry-breaking QPT in insulators are reasonably well understood by now, with agreement between experiment and theory. In contrast, transitions in metals remain only partially understood [3, 4]. Moreover, and most relevant to this chapter, recent developments in the field of frustrated and topological systems have brought into focus entirely new forms of quantum criticality which are under intense investigation today [5]. For some of them, microscopic ingredients beyond the simplest non-relativistic single-orbital picture are crucial, defining an extremely fruitful and rich avenue of research.

In the following, we will focus on interacting electrons in solids and thus on collective phenomena. In contrast, we will not cover transitions driven by the topology of band electrons; similarly, we will not be concerned with transitions driven by quenched disorder. Our primary interest is on thermodynamic and linear-response spectral properties of systems in the vicinity of a QPT. The non-equilibrium quantum dynamics near QPTs as well as genuine non-equilibrium phase transitions have become an intense research field on its own, but are beyond the scope of this chapter.

Given the complexity of material, we will mainly discuss conceptual ideas and qualitative aspects of theory; for concrete computations we refer the reader to the literature. Experimental results will be mentioned when appropriate.

2 Quantum phase transitions

Before turning to frustration, orbitals, and the like, we will summarize the main aspects of "conventional" quantum criticality. For reasons of space, this review can be nowhere close to complete. However, many extensive texts on this subject are available [3, 4, 6] which we refer the reader to for a more detailed exposure.

2.1 Phenomenology and Landau-Ginzburg-Wilson theory

A quantum phase transition (QPT) is a phase transition taking place at temperature $T = 0$ upon tuning a non-thermal control parameter like pressure or magnetic field. The finite-temperature properties near a continuous QPT are highly unusual: Due to the peculiar properties of the quantum ground state at the transition point, dubbed quantum critical point (QCP), the so-called quantum critical regime located at finite T above the QCP, Fig. 1, displays properties distinct from that of any stable phase of matter. These properties include power-law behavior with

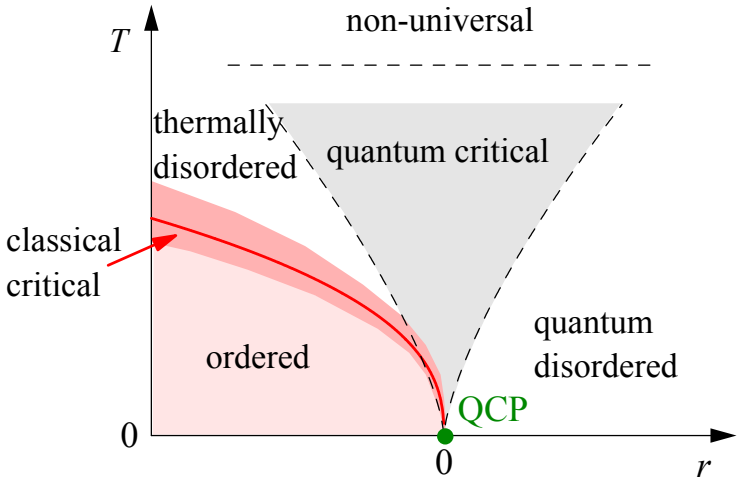

Fig. 1: *Generic phase diagram in the vicinity of a quantum critical point as function of a non-thermal control parameter r and temperature T. An ordered phase exists for $r < 0$ and low T, bounded by a line of classical phase transitions which terminates at the QCP at $r = 0$, $T = 0$. The quantum critical regime is defined by $k_B T \gg |r|^{\nu z}$, where ν and z are the correlation length and dynamical exponents.*

unconventional exponents of thermodynamic and transport quantities as function of absolute temperature as well as scaling behavior, where suitably rescaled observables depend only on dimensionless ratios of external parameters.

From a theoretical perspective, the universal properties of QPTs can often be described using a continuum quantum field theory for the transition's order parameter. The choice of the latter is dictated by the way in which symmetries of the Hamiltonian are spontaneously broken at the transition. This goes back to Landau who pioneered the ideas of symmetry breaking and local order parameters in the context of phase transitions. This concept was later extended to quantum phase transitions by taking into account temporal order-parameter fluctuations, i.e., quantum fluctuations – this leads to the so-called Landau-Ginzburg-Wilson (LGW) approach.

For Mott-insulating quantum magnets the LGW theory for a zero-temperature transition between a featureless paramagnet and, e.g., a collinear ordered antiferromagnet takes the form of a quantum φ^4 model with the action

$$\mathcal{S} = \int d^d x \int_0^\beta d\tau \left(\frac{c_0^2}{2} (\partial_i \vec{\varphi})^2 + \frac{1}{2} (\partial_\tau \vec{\varphi})^2 + \frac{\delta_0}{2} \vec{\varphi}^2 + \frac{u_0}{4!} (\vec{\varphi}^2)^2 \right) \tag{1}$$

where $\partial_i = \partial/\partial x_i$, and $\vec{\varphi}(\vec{x}, \tau)$ is a local N-component order-parameter field which is assumed to vary slowly in space and time and encodes the ordering tendency at a microscopic wavevector $\vec{Q}$. Further, τ is imaginary time, and c_0, δ_0, and u_0 are parameters. Decreasing the non-thermal control parameter δ_0 at low temperature tunes a transition between a disordered and an ordered phase, with the O(N) symmetry spontaneously broken in the latter; $N = 3$ for collinear Néel order in the presence of SU(2) spin symmetry. More precisely, δ_0 acquires a temperature-dependent renormalization, and the transition occurs at $\delta_0 = \delta_c$ where the renor-

malized δ vanishes. The distance to the QCP can be expressed as

$$r = \delta_0 - \delta_c(T{=}0) \tag{2}$$

and may be tuned by pressure or chemical composition. Eq. (1) can also describe non-magnetic ordering transitions, such as the onset of charge order accompanied by the breaking of lattice translation symmetry.

The thermodynamic properties of Eq. (1) are essentially understood, as they can be computed analytically using renormalization-group techniques as well as numerically. The critical exponents of the QPT are known to a good accuracy in all space dimensions. Similarly, dynamical and spectral properties have been considered, and a detailed exposition is given in Ref. [3].

In Eq. (1) space and time enter symmetrically, corresponding to a dynamical exponent $z = 1$. The time direction in the integral may be interpreted as an additional space direction, such that the quantum theory in d dimensions at $T = 0$ is equivalent to a classical theory in $D = d + z$ dimensions. While the local order-parameter description with $z = 1$ applies to many QPT in insulators, the situation in metals is more complicated due to the presence of low-energy fermionic excitations. Two additional remarks are in order: (i) QPTs into ferromagnetic or polarized phases in the presence of SU(2) spin symmetry follow a quantum dynamics different from that of the φ^4 model because a *conserved* density changes across the transition. (ii) Berry-phase terms, which are generically present in a field-theory description of spin systems, do not appear in Eq. (1) because they are irrelevant for the transition between featureless paramagnet and antiferromagnet. They are, however, responsible for much of the physics beyond LGW which will be described in Sec. 6.

For finite-temperature (i.e. classical) transitions, the upper critical dimension above which mean-field critical behavior is realized is $D_c^+ = 4$ for a standard φ^4 theory. In the quantum case, the presence of temporal fluctuations implies that the upper critical dimension for QPTs is given by $d_c^+ = 4{-}z$. For instance, continuous QPTs in $d{=}3$ with $z{=}1$ display mean-field behavior with logarithmic corrections. For phase transitions involving fermions the situation may be more complicated, though.

A last parenthetical remark here: Zero-temperature phase transitions, both continuous and discontinuous, can also occur in purely classical models. Obvious examples occur classical models of vector spins: For instance, the field-driven transition to saturation in a classical Heisenberg model is typically continuous.

2.2 An example: Coupled dimers and $TlCuCl_3$

A class of simple microscopic models displaying magnetic QPTs is given by coupled dimers, i.e., lattice systems with a crystallographic unit cell containing two spins $1/2$. Consider the Heisenberg Hamiltonian

$$H = J \sum_{\langle ij \rangle} \vec{S}_i \cdot \vec{S}_j + \lambda J \sum_{\langle ij \rangle'} \vec{S}_i \cdot \vec{S}_j \tag{3}$$

where the first sum runs over all dimers, whereas the second sum covers all inter-dimer bonds. A square-lattice realization is shown in Fig. 2. The limit $\lambda = 0$ corresponds to disconnected

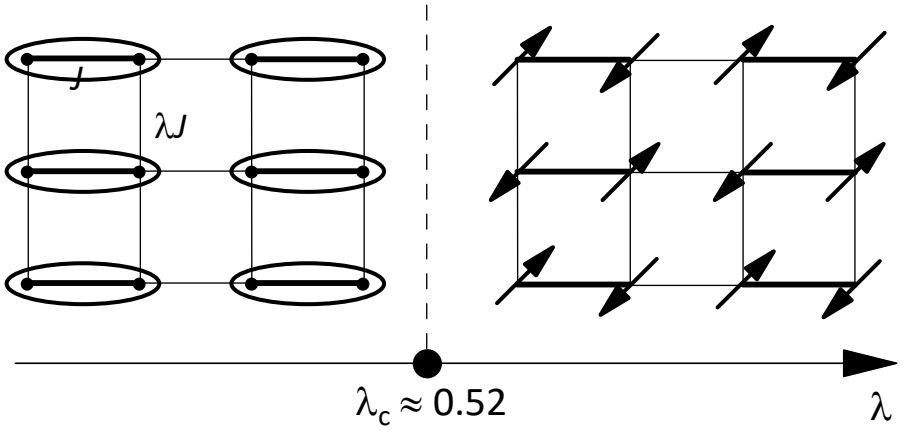

Fig. 2: *Square-lattice coupled-dimer model* (3) *with phase diagram: The two Heisenberg coupling J and λJ are shown as thick and thin lines, respectively. The ellipsoids represent singlet pairs of spins $1/2$. At a critical value λ_c the system transits from a gapped singlet paramagnet (left) to a Néel antiferromagnet (right).*

spin pairs, each of them having a singlet $S = 0$ ground state and a triplet $S = 1$ excited state, separated by an excitation energy J. The full lattice model has two distinct phases, which can be easily discussed:

Limit $\lambda \ll 1$: This implies weakly coupled dimers, leading to a disordered (i.e. quantum paramagnetic) phase with no broken symmetries and exponentially decaying spin correlations.

Limit $\lambda \sim 1$: Here the dimers are strongly coupled, and long-range antiferromagnetic order with broken SU(2) symmetry emerges. For the lattice shown in Fig. 2, $\lambda = 1$ represents a square lattice which is known to display long-range order.[1]

A quantum phase transition must occur at an intermediate value of λ, Fig. 2. As the order parameter is the staggered magnetization, the QPT is described by the LGW theory (1) with $N = 3$ components. The excitation gap of the quantum paramagnet closes upon approaching the QCP. The ordered phase displays two gapless Goldstone modes corresponding to the broken spin rotation symmetry as well as a gapped Higgs mode corresponding to amplitude fluctuations of the order parameter.

A paradigmatic experimental realization of coupled dimers, here in three space dimensions, is found in the Mott-insulating material $TlCuCl_3$ [7]. The magnetic Cu ions form dimers, and at ambient pressure and low temperature the material is in the quantum paramagnetic phase. Upon applying hydrostatic pressure, the inter-dimer interactions increase (i.e. λ in Eq. (3) increases) such that the system eventually reaches a state with antiferromagnetic long-range order. Ignoring the (weak) spin-orbit coupling, the QPT between the two states is described by the LGW theory (1) as above. Given that $D = d + z = 4$, the QPT is of mean-field character.

[1] The system in Fig. 2 becomes disordered again for $\lambda \gg 1$, as this limit corresponds to decoupled spin ladders.

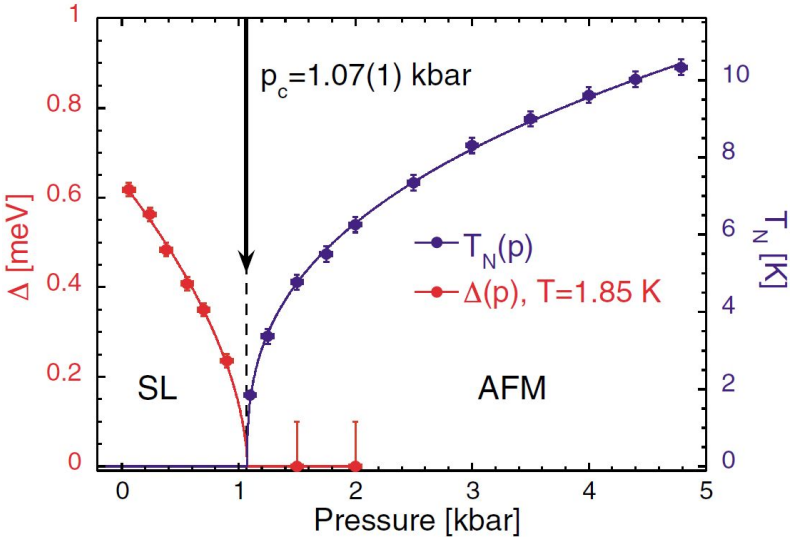

Fig. 3: *Experimental results for the coupled-dimer system $TlCuCl_3$, showing the magnetic excitation gap Δ and the Néel temperature T_N as function of applied pressure p. The magnetic QPT is located at $p_c = 1.07$ kbar. (Figure taken from Ref. [7])*

2.3 Frustrated systems: What is different?

The considerations so far cover "simple" symmetry-breaking transitions, i.e., transitions between a symmetric – and also otherwise featureless – state and a state which can be characterized by a local order parameter and spontaneously breaks one or more symmetries of the Hamiltonian. While such transitions can of course also occur in frustrated systems, more complicated situations frequently arise which cannot be captured by a simple LGW theory. Important cases are:

1. If a quantum paramagnetic phase is a fractionalized spin liquid, it is *not* featureless, because it is characterized by topological order.

2. The ordered-state manifold may be unconventional, i.e., not be characterized by a local order parameter or by a unique ordering wavevector. Long-range order may arise exclusively from fluctuation effects.

3. A transition might occur between states without spontaneous symmetry breaking.

4. The active quantum degrees of freedom can be different from the fluctuations of the order parameter, i.e., if a local order parameter exists, it might be a composite when expressed in the elementary degrees of freedom.

5. Frustration may enhance fluctuations such that the transition is rendered first order.

In Sec. 5 and 6 we will cover some of these cases in more detail.

3 Frustration and novel states

Frustration refers to the presence of multiple constraints which cannot be simultaneously satisfied. An important arena is frustrated magnetism where the constraints arise from the minimization of (pairwise) interaction energies: In a frustrated magnet, not all interactions can be simultaneously minimized. The perhaps simplest example is given by antiferromagnetically coupled Ising spins on a triangle. Frustration can arise from the geometry of the underlying lattice and/or from the nature of the interactions. The most obvious effect of frustration is to counteract the usual tendency towards symmetry-breaking order at low temperatures. As a result, a frustrated system may either have a strongly reduced ordering temperature or show no order at all, the latter often leading to exotic liquid-like phases. In addition, the suppression of conventional ordering phenomena can induce a competition of multiple less conventional phases, resulting in complex phase diagrams, non-trivial crossover phenomena, an accumulation of entropy at low temperature, and a large sensitivity to tuning parameters.

The past decade has seen a flurry of interest in frustrated systems [8–13], primarily driven by the search for novel states of matter. Prime examples are spin liquids with fractionalized degrees of freedom, skyrmion lattices with emergent artificial electrodynamics, fractionalized Fermi liquids, and their descendants. Many of these phases are characterized by non-trivial topological properties.

In this section, we introduce important concepts for frustrated magnets. The discussion here will focus on Mott insulators with local moments; frustrated metals define a large separate topic on its own, and we will only touch upon this in Sec. 7. We will consider lattice systems of local moments, i.e., quantum-mechanical spins transforming as SU(2) vectors, with a Hamiltonian containing two-spin interactions plus, perhaps, multi-spin exchange terms. The most generic model Hamiltonian is an antiferromagnetic Heisenberg model of spins S with nearest-neighbor interactions J,

$$\mathcal{H} = J \sum_{\langle ij \rangle} \vec{S}_i \cdot \vec{S}_j \,. \tag{4}$$

The Heisenberg interaction in Eq. (4) favors antiparallel moments on neighboring lattice sites. Consequently, this interaction is non-frustrated on lattices where all closed loops of interaction paths have even length, such that an alternating up–down arrangement, corresponding to collinear magnetic order, can cover the lattice. This applies to the square and cubic lattices as well as, e.g., the honeycomb lattice. In contrast, frustration is induced on lattices with odd-length loops, e.g., the triangular, kagome, bcc, fcc, and pyrochlore lattices. On some of these lattices, a magnetically ordered ground state – often non-collinear – is realized for any S despite the existence of frustration, the triangular lattice with its 120° order being an established example, while in other cases order may be entirely absent.

In addition to the described *geometric frustration*, rooted in the geometry of the underlying lattice, incompatible constraints may be caused by the nature of the exchange interactions, leading to *exchange frustration*. A prominent case are so-called Kitaev interactions [14], to be described in Sec. 4 below.

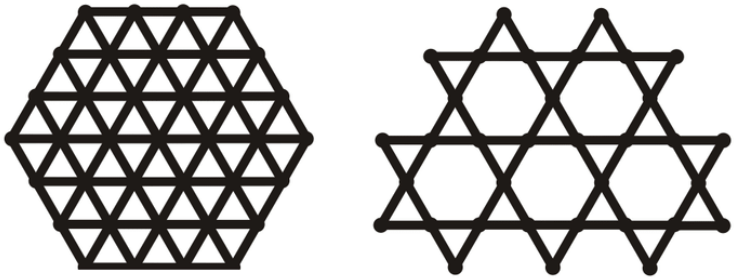

Fig. 4: *Two-dimensional lattices with geometric frustration: triangular (left), kagome (right).*

Given that frustration tends to suppress magnetic order, a popular experimental way to quantify frustration in a given system is the so-called frustration ratio, $f = |\Theta_{\rm CW}|/T_{\rm N}$, where $T_{\rm N}$ is the ordering temperature and $\Theta_{\rm CW}$ the Curie-Weiss temperature, the latter being a measure for the strength of exchange interactions [8]. Materials with $f > 5$ are commonly called "frustrated". The extreme case of no long-range order (LRO) down to $T = 0$, formally $f = \infty$, then corresponds to a ground state with only short-range correlations. A regime with highly correlated but fluctuating spins and no LRO at temperatures $T \ll |\Theta_{\rm CW}|$ is often dubbed "spin liquid" (although more precise definitions are available, see below).

3.1 Classical spin liquids

In the classical limit, formally obtained for spin size $S \to \infty$, spins can be viewed as unit vectors, and non-trivial commutators vanish. Frustration may lead to a classical ground state which is either unique up to global symmetry transformations – in this case the system is called "weakly frustrated" – or which has degeneracies scaling with the system size, rendering the system "strongly frustrated".[2] In the latter case, the resulting manifold of lowest-energy states defines a *classical spin liquid*. A celebrated example is spin ice, referring to moments with local Ising anisotropy and ferromagnetic interactions on a pyrochlore lattice, viz. a lattice of corner-sharing tetrahedra [15].

Often, a classical spin liquid can be characterized by a set of local conditions which define the ground-state manifold (but *not* a unique state up to global symmetry transformations, as explained above). Examples are the conditions "two in, two out" for the Ising configurations of individual tetrahedra of spin ice or the condition $\sum_\triangle \vec{S}_i = 0$ for the spin configurations of a kagome-lattice Heisenberg model. Hence, these conditions *underconstrain* the manifold of states; recall that the original problem of minimizing all Hamiltonian terms simultaneously *overconstrains* the manifold of states if frustration is present. Local constraints can often be formulated as an emergent lattice gauge theory. For instance, the "two in, two out" condition can be translated into $\mathrm{div}\, b = 0$ where b is an artificial magnetic field and div a suitably defined lattice divergence.

For Ising spins (i.e. with countable number of states) a classical spin liquid can be characterized by an extensive ground-state entropy S_0/N where N is the number of lattice sites. Typical

[2] Intermediate cases with sub-extensive degeneracies exist as well.

examples are the Ising model on a triangular lattice, with $S_0/(Nk_B) \approx 0.323$ [16], and classical spin ice, with $S_0/(Nk_B) \approx 1/2\ln(3/2) \approx 0.203$ [17]. For classical spin liquids made from XY or Heisenberg spins a residual entropy cannot be defined, but the degeneracy may be quantified via the difference between the number of continuous degrees of freedom and the number of local constraints.

Elementary excitations of classical spin liquids correspond to configurations which violate one (or more) of the local ground-state conditions; in the gauge-theory language these become elementary charges. For spin ice, the excitations are tetrahedra with "three-in, one-out" or "one-in, three-out" configurations; these have been shown to behave like magnetic monopoles upon including dipolar interactions [18].

3.2 Quantum spin liquids

With quantum fluctuations included, frustrated systems may realize local-moment states without symmetry breaking and only short-range order down to lowest temperatures. Such quantum spin liquids (QSLs) [9,11,12] display some differences compared to their classical counterparts: (i) Quantum fluctuations typically remove the extensive ground-state degeneracy of strongly frustrated systems by quantum tunnelling, resulting in unique ground states (up to global symmetry transformations or topological degeneracies). (ii) QSLs are thermodynamically stable phases of matter, characterized by emergent dynamic gauge fields and topological order. This implies the existence of fractionalized excitations which are coupled to the gauge field. Despite this coupling, the fractionalized excitations are asymptotically free, i.e., deconfined. (iii) The wavefunctions of QSLs can be characterized by long-range entanglement [19,20]. Importantly, QSLs need to be distinguished from "trivial" quantum paramagnets without topological order and fractionalization, like the coupled-dimer magnets of Sec. 2.2.

Different types of QSLs can be distinguished depending on the spectrum and statistics of the emergent excitations and on the gauge structure. Prominent examples are fully gapped $\mathbb{Z}_2$ spin liquids, for which topological order can be sharply defined, and algebraic U(1) spin liquids with gapless excitations. For an in-depth discussion of topological order and attempts of classifications we refer the reader to the literature [9, 11, 21]. Relevant to the existence of non-trivial many-body states is a theorem due to Lieb-Schulz-Mattis [22] and its higher-dimensional generalization by Hastings [23]. It states that in a system with half-odd-integer spin per unit cell and global U(1) symmetry, the excitation spectrum in the thermodynamic limit cannot simultaneously fulfill the two conditions: (a) the ground state is unique and (b) there is a finite gap to all excitations. This implies that a gapped symmetry-unbroken state must have a ground-state degeneracy which is topological in nature. We finally note that, conceptually, topological order and fractionalization may co-exist with spontaneous symmetry breaking: For instance, broken time-reversal symmetry on top of a spin liquid leads to a chiral spin liquid, while magnetic long-range order leads to a fractionalized ordered magnet.

An intuitive picture of a QSL with underlying SU(2) symmetry is provided by the resonating valence-bond (RVB) idea, Fig. 5, originally proposed by Anderson for the triangular-lattice

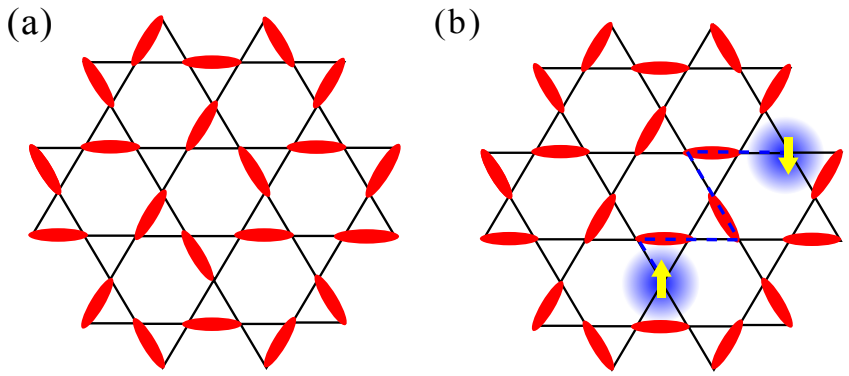

Fig. 5: *Illustration of an RVB state, here on the kagome lattice. (a) Nearest-neighbor dimer covering, with the ellipsoids representing singlet pairs of spins* $1/2$*. The RVB state is given by an equal-weighted superposition of different such coverings. (b) Pair of spinon excitations, each carrying spin* $1/2$*.*

Heisenberg model [24]. RVB refers to pairing spins on a lattice into singlets and then forming a quantum superposition of many different pairings, i.e., different dimer coverings of the lattice, such that the symmetries of the Hamiltonian are preserved.[3] This picture captures the aspect of fractionalized excitations, as the breaking of a dimer leads to two monomer excitations with independent dynamics: These monomers are objects carrying charge 0 and spin $1/2$, typically called *spinons*. In a $\mathbb{Z}_2$ spin liquid, they are coupled to an emergent $\mathbb{Z}_2$ gauge field, whose excitations are $\mathbb{Z}_2$ vortices (or fluxes) called *visons*.

A well-studied spin model with geometric frustration is the Heisenberg model on the kagome lattice. For quantum spins $1/2$, with antiferromagnetic interactions as in Eq. (4), there is strong numerical evidence that this realizes a fractionalized QSL. However, the nature of this QSL has not been conclusively clarified to date, as numerical results have been interpreted in favor of either a gapped $\mathbb{Z}_2$ spin liquid [26] or a U(1) spin liquid with a Dirac-cone spectrum [27, 28]. A candidate material realizing the kagome-lattice spin-$1/2$ Heisenberg model is Herbertsmithite, $ZnCu_3(OH)_6Cl_2$, which indeed displays spin-liquid-like behavior [29, 30]. However, the role of quenched disorder is debated [30]. Numerical evidence for QSL phases in Heisenberg models of spins $1/2$ has also been found for square [31] and triangular-lattice models [32] with first and second-neighbor interaction, so-called J_1-J_2 models. Close experimental realizations of the triangular-lattice J_1-J_2 model appear in the delafossite family $NaYbX_2$ ($X=$ S, Se, O) which show spin-liquid behavior at low T [33, 34].

3.3 Valence-bond solids

An alternative quantum paramagnetic state of spins $1/2$ that can be constructed from dimer coverings of the underlying lattice is a so-called valence-bond solid (VBS). In this state, the wavefunction is dominated by a single covering with a periodic arrangement of dimers. As a

[3] The first existence proof of a $\mathbb{Z}_2$ spin liquid was given for a triangular-lattice quantum dimer model which realizes an RVB phase [25].

result, the state spontaneously breaks translation and rotation symmetry of the lattice, hence the label *solid*. Excitations of VBS states carry integer spin, i.e., spinons are confined.
VBS variants can be constructed for larger constituent spins and/or from larger units, the common theme being that the state in the resulting magnetic unit cell represents a spin singlet. For instance, plaquette VBS with unit cells of four spins $1/2$ have been discussed for the square-lattice checkerboard and J_1-J_2 models.

3.4 Order by disorder and unconventional types of order

In addition to phases with unbroken spin symmetry, like spin liquids and valence-bond solids, frustrated spin systems can of course display phases with broken spin symmetry, both conventional and unconventional [13].
First, conventional magnetic order can emerge in an unconventional way. Most prominent is so-called "order by disorder" which refers to a situation where a frustration-induced degeneracy of the classical ground-state manifold is lifted by fluctuations, either thermal or quantum [35]. A well-studied example is the easy-plane pyrochlore antiferromagnet, where long-range order emerges due to fluctuations from a one-parameter manifold of classically degenerate states [36].
Second, less conventional magnetic order can appear as a result of large crystallographic unit cells or non-Heisenberg interactions. Among the possibilities are so-called multi-Q states where the ordering pattern results from the superposition of modulations with multiple inequivalent wavevectors, among which skyrmion lattices have attracted particular attention [37].
Third, ordered states may spontaneously break spin symmetry not by dipolar order, but by order in higher multipole channels. The simplest form is quadrupolar or spin-nematic order which breaks SU(2) symmetry and is described by a local rank-2 tensor order parameter [38,39]. Such order is known to be realized in certain spin-1 Heisenberg models with additional biquadratic interactions [40].

4 More ingredients: Orbitals and spin-orbit coupling

While the Heisenberg model provides a useful and rich arena for quantum magnetism, the description of real materials often requires to include physics beyond. Two important ingredients are spin-orbit coupling (SOC) and orbital degrees of freedom, which we discuss in turn.

4.1 Magnetic anisotropies and novel forms of frustration

In the non-relativistic limit, SOC is not present, implying that real space and spin space are entirely separate, with SU(2) spin rotation symmetry in the absence of a magnetic field. In contrast, non-vanishing SOC couples real space and spin space, such that symmetry transformations in general act on both position and spin. Consequently, the symmetry of spin–spin interactions in a solid is lowered (compared to Heisenberg) and is dictated by the lattice structure. The simplest forms of anisotropic interactions are (i) Ising, $S_i^z S_j^z$, (ii) XY, $S_i^x S_j^x + S_i^y S_j^y$,

and (iii) Dzyaloshinskii-Moriya $\vec{D}_{ij} \cdot (\vec{S}_i \times \vec{S}_j)$. The latter is antisymmetric under exchange $i \leftrightarrows j$ and hence requires broken inversion symmetry to exist; this does not apply to the former.

In addition to anisotropic interactions, magnetic anisotropies may also arise at the single-ion level. Such single-ion anisotropies are rooted in the orbital character of the magnetic state, combined with SOC. A common single-ion term in the Hamiltonian is $D{S_i^z}^2$, where $D > 0$ ($D < 0$) corresponds to an easy-plane (easy-axis) anisotropy, respectively. On a non-Bravais lattice, different sites can have distinct *local* anisotropy axes.

Importantly, magnetic anisotropies enable forms of frustration different from that of Heisenberg models. Some of those have already been mentioned above: An easy-axis anisotropy on the pyrochlore lattice, combined with ferromagnetic interactions, leads to spin-ice behavior. The corresponding easy-plane situation results in a U(1) classical degeneracy and order by disorder.

Anisotropic interactions may even induce frustration on lattices whose geometry is unfrustrated. Such exchange frustration is the key ingredient for the route to QSLs proposed by Kitaev [14]. The Kitaev honeycomb model features bond-dependent Ising interactions,

$$\mathcal{H} = -J^x \sum_{\langle ij \rangle_x} S_i^x S_j^x - J^y \sum_{\langle ij \rangle_y} S_i^y S_j^y - J^z \sum_{\langle ij \rangle_z} S_i^z S_j^z \tag{5}$$

where the bonds of the underlying honeycomb lattice have been divided into three sets of mutually parallel bonds, labeled $\alpha = x, y, z$, and $\langle ij \rangle_\alpha$ refers to a summation over the bonds of α type. The Kitaev model has attracted tremendous attention, as it realizes an exactly solvable $\mathbb{Z}_2$ spin liquid whose emergent excitations are Majorana fermions and static $\mathbb{Z}_2$ gauge fluxes. It has been subsequently generalized to other lattices and space dimensions [41]. Experimentally, strong Kitaev interactions on the honeycomb lattice have been deduced for the materials α-$RuCl_3$ [42, 43], Na_2IrO_3 [44, 45], and various polytypes of Li_2IrO_3 [46–48]; however, all of these materials display magnetic LRO at low temperatures due to the presence of additional interactions.

4.2 Orbitals and spin-orbital liquids

The ground state of ions with partially filled shells may contain, in addition to spin degrees of freedom, also orbital degrees of freedom. The latter arise from orbital degeneracies which themselves depend on the crystalline electric field arising from the potential of the surrounding ions. For example, Cu in octahedral coordination may realize a $3d^9$ configuration, with one hole in doubly degenerate e_g orbitals, leading to $S = 1/2$ spin and $\tau = 1/2$ orbital degrees of freedom. More complicated is V in a cubic environment with a $3d^2$ configuration in triply degenerate t_{2g} orbitals, resulting in $S = 1$ (by Hund's rule) and $\tau = 1$.

Insulators with orbital degrees of freedom require to write down spin-orbital exchange models [49]. While these are typically complicated and have low symmetry, reflecting the influence of both lattice and orbital structure on exchange processes, a qualitative understanding can often be gained by simpler more symmetric models. An example is the SU(4)-symmetric Kugel-

Khomskii model,

$$\mathcal{H} = J \sum_{\langle ij \rangle} (\vec{S}_i \cdot \vec{S}_j + \frac{1}{4})(\vec{\tau}_i \cdot \vec{\tau}_j + \frac{1}{4}), \tag{6}$$

with $\vec{\tau}_i$ representing the orbital degrees of freedom. While such spin-orbital models often exhibit phases with coexisting orbital and magnetic order, it has been suggested early on that, if combined with either geometric frustration or exchange frustration, they may also produce low-temperature states devoid of symmetry breaking in both the spin and orbital sector. Such states have consequently been dubbed spin-orbital liquids [50]. Indeed, the bond-dependent interactions of the Kitaev honeycomb model can be used to construct an exactly solvable model for a spin-orbital liquid [51].

5 Conventional quantum criticality in frustrated systems

Quantum phase transitions in frustrated magnetic insulators may be conventional in the sense that they involve symmetry breaking and local order parameters. Less conventional cases involving fractionalization and topology will be postponed to the next section.

5.1 Magnetic ordering transitions

The simplest case, a quantum transition from a featureless paramagnet to a symmetry-broken phase with antiferromagnetic or VBS order, is expected to be described by an LGW theory of φ^4 type, Eq. (1), with dynamical exponent $z = 1$. Symmetry and wavevector of the order parameter determine the effective number of order-parameter components and the structure of the interaction terms in the field theory.

Frustration enters in a non-trivial way, because the order-parameter structure of non-collinear or non-coplanar states is much richer than that of simple collinear magnets. Most straightforwardly, this translates into a larger number of components N in the corresponding φ^4 theory. This is not all: For instance, a non-collinear ordered state often breaks both SU(2) spin rotation symmetry and a $\mathbb{Z}_2$ chiral symmetry, and both symmetries can be broken either in a single or in two separate transitions. For the classical case, this has been studied for stacked triangular-lattice Heisenberg antiferromagnets: Monte Carlo simulations have observed a single transition with non-trivial critical exponents, different from that of standard O(N) universality, consistent with a proposal by Kawamura [52].[4] Numerical results for the quantum case are, to our knowledge, not available due to the notorious sign problem.

More seriously, frustration can render invalid the concept of discrete well-defined wavevector for critical fluctuations: Upon approaching an ordered state, fluctuations may become soft on a manifold of wavevectors, e.g., owing to frustration-induced degeneracies. Strong fluctuation effects may then cause the transition to be first order. Alternatively, exotic novel intermediate

[4] More recent theory works predict the transition in stacked triangular-lattice Heisenberg antiferromagnets to be weakly first order [53].

phases might emerge. An interesting open problem in this context constitutes the quantum melting of a skyrmion crystal [37]. Such a phase has been observed in a number of helical magnets. One prominent material is MnSi where the lack of inversion symmetry enables Dzyaloshinskii-Moriya interactions to produce long-wavelength helical order which in turn yields a skyrmion crystal in a small window of magnetic field and temperature [54]. In MnSi, long-range magnetic order can be suppressed by the application of pressure, giving way to an extended non-Fermi liquid phase at low temperature [55]. It has been speculated that this behavior is related to partial order, e.g., a skyrmion liquid, but a concise theory is not known.

A further complication, frequently present in strongly frustrated systems, arises due to order-by-disorder physics (Sec. 3.4): If the actual ordered state is selected by fluctuation effects from a larger (e.g. classically degenerate) manifold, then some or all properties of the transition may be determined by the larger symmetry of this manifold. This type of physics is known from $\mathbb{Z}_n$ clock models, or alternatively XY models with $\mathbb{Z}_n$ anisotropy. Here, anisotropies with $n \geq n_c$ are irrelevant at criticality, such that the critical behavior is that of the XY model. For $d = 2$ (or $D = 1 + 1$) this even changes the phase diagram, as an intermediate critical phase intervenes between the disordered and the $\mathbb{Z}_n$-ordered phases for $n \geq 5$ [56]. An example of recent interest are the finite-temperature intermediate phases present in the two-dimensional (2D) Heisenberg-Kitaev model [57] where the relevant ordered phases are sixfold degenerate as a result of Kitaev interactions reflecting spin-orbit coupling [58]. Theoretical results for the *quantum* phase transitions in this model indicate first-order behavior both on analytical [59] and numerical [60, 61] grounds, but the numerics has not reached conclusive accuracy yet.

Strong frustration may, in addition, lead to *dimensional reduction*: This refers to a situation where the effective spatial dimension of the order-parameter fluctuations is smaller than that expected from the microscopic model. For instance, a three-dimensional (3D) layered system with inter-layer frustration may display 2D critical behavior. Such dimensional reduction typically does not reach down to lowest energies and temperatures, due to residual higher-dimensional couplings, such that a dimensional crossover to fully 3D critical behavior at lowest temperatures occurs [62].

5.2 Field-driven transitions and BEC phenomena

Local-moment magnets can display a variety of QPTs as function of applied magnetic field. The simplest case is the transition at the saturation field of an SU(2)-symmetric Heisenberg magnet: Upon lowering the field, a high-field magnon becomes soft at a particular wavevector, and the transition can be understood as magnon Bose-Einstein condensation (BEC) which turns the fully polarized state into a canted antiferromagnet. The latter breaks the U(1) spin rotation symmetry about the field axis and is therefore also understood as a spin superfluid. The boson condensation nature of the QPT implies that this is in the universality class of the dilute Bose gas, with $z = 2$ [3]. A similar field-driven transition occurs between the low-field singlet and intermediate-field canted phases of the coupled-dimer magnets of Sec. 2.2 [63].

While these transitions involve only trivial magnetization plateaus at $M/M_{\rm sat} = 0$ and 1, frus-

trated magnets often display intermediate magnetization plateaus. The QPTs in and out of such a magnetization plateau may be of BEC type, but are more complicated if the plateau phase spontaneously breaks lattice translation symmetry. Then, the plateau phase and the adjacent canted phase break different symmetries, possibly resulting in two continuous transitions with an intermediate coexistence (i.e. supersolid) phase or a first-order transition [64]. Experimentally, such field-induced supersolidity has been discussed for the Shastry-Sutherland compound $SrCu_2(BO_3)_2$ [65] and for the spinel $MnCr_2S_4$ [66].
Strong frustration often renders the magnon bandwidth small, paving the way for more exotic field-driven transitions. As has been discussed for a variety of frustrated Heisenberg models, it is possible that the high-field phase displays multi-magnon bound states whose minimal energy lies below that of the single-magnon branch. Then, upon lowering the field, the first instability is in this multi-magnon sector, and the resulting ordered state can be understood as a condensate of magnon bound states [67]. The most important case is that of two-magnon bound states whose condensation induces a spin-nematic state: This is a state with quadrupolar order whose order parameter is a traceless rank-2 tensor. The QPT from the high-field state is either continuous of BEC type, with $z = 2$, or is of first order due to large fluctuations.
Last not least, we note that spin-orbit coupling drastically modifies the physics described above. First, magnetization is no longer conserved, such that the fully polarized state is not an eigenstate of the Hamiltonian. As a result, the magnetization in the high-field phase is not saturated even as $T \to 0$. Second, the lower symmetry typically implies that field-driven transitions break discrete symmetries only. The corresponding QPT are then of $\mathbb{Z}_n$ type, with dynamic exponent $z = 1$. For instance, this applies to the Kitaev material α-$RuCl_3$: Although its field-induced phases are not fully understood to date, it is clear that the magnetization in the asymptotic high-field phase receives substantial quantum corrections [68], and it can be expected that the QPT to the asymptotic high-field phase is either of Ising type or of first order.

6 Transitions involving topological states

Phase transitions in and out of topologically non-trivial states (more precisely, states with intrinsic topological order) can in general not be captured by LGW theory, as topology is associated with global instead of local properties. Nevertheless, topological states and their transitions can often be described by local quantum field theories which then involve novel emergent degrees of freedom coupled to gauge fields. We will discuss a few of such transitions in turn.

6.1 Confinement transitions and fractionalized criticality

QPTs in and out of topological liquid states are fundamentally different from the conventional transitions, as they necessarily involve the fractionalized degrees of freedom of the (spin) liquid. In many cases, these are spinons (i.e. fractionalized constituents of the microscopic spins) and excitations of the emergent gauge field in its deconfined phase. Continuous transitions out of a spin liquid can often be understood as a condensation transition of one of these particles (or

bound states thereof) [11, 69]. Physical spins are then composite objects in terms of the critical degrees of freedom. As a result, spin correlation functions display critical power laws with *large* anomalous exponents: While standard O(N) universality yields numerically small anomalous exponents, e.g. $\eta = 0.06$ for the 3D Heisenberg model, many of the exotic transitions discussed below have η values for physical correlators of order unity.

Starting from a fractionalized spin liquid, one can envision the following options for QPTs: (i) a confinement transition to a featureless paramagnet, (ii) a confinement transition with concomitant symmetry breaking, leading to e.g. magnetic or VBS order – typically these are Higgs-type transitions driven by the condensation of a particle with gauge charge, (iii) a condensation transition which leaves the deconfinement intact, which then leads to exotic fractionalized magnetic (AF*) or VBS states (VBS*), (iv) a transition to a different fractionalized spin liquid.

In the following, we list a few examples from the theory literature. The field theories are typically written down in terms of fractionalized particles coupled to gauge fields (a simple example being the CP^1 model (7) specified below); in some cases topological quantum field theories (most importantly, Chern-Simons theories) have also proven useful. Most considerations apply to two space dimensions; less work has been done for $d = 3$.

Transitions in group (i) require the presence of a featureless paramagnetic phase in addition to a topological spin liquid: The former can be realized, e.g., by application of a magnetic field or by the formation of singlet dimers as in bilayer models. A concrete example is the 2D toric-code model [70] in a longitudinal field [71]: It displays a continuous transition from a $\mathbb{Z}_2$ topological spin liquid to a featureless high-field phase. The transition has been shown to be in the Ising* universality class in $D = 2 + 1$ dimensions [72]. Here, Ising* refers the fact that the critical degrees of freedom have Ising symmetry, but are very different from a conventional order parameter, as they derive from the fractionalized excitations of the spin liquid. Hence, thermodynamic properties are that of Ising criticality in $D = 2 + 1$, but correlation functions of physical spins strongly differ from the conventional case as spins are composite objects here. This can be expected to generically apply to confinement transitions of $\mathbb{Z}_2$ spin liquids. A second example is the ferromagnetic honeycomb-lattice Kitaev model in a magnetic field [73, 74]: This displays a single transition between a $\mathbb{Z}_2$ spin liquid and a featureless high-field phase as well, Fig. 6. However, it is open whether this transition is weakly first order or continuous.

Transitions in group (ii) have been mainly discussed within effective field theories, and candidate models are known in many cases. A typical situation is that of vison condensation in a 2D $\mathbb{Z}_2$ spin liquid; if the vison has non-trivial transformation properties under lattice symmetries, its condensation generically breaks translation symmetry and induces VBS order. Such transitions have been argued to be of O(N)* type (where * again refers to the fact that the primary fields are fractionalized) – supplemented by lattice anisotropy terms which are irrelevant at criticality – where the number of components N of the vison-derived field depends on the lattice and the resulting VBS state. For example, the transition to a columnar VBS on both the square and honeycomb lattices is of 3D XY* type [25, 75, 76], while on the triangular lattice the transition to a columnar VBS is proposed to be of 3D O(6)* type [77]. In contrast, transitions to staggered VBS

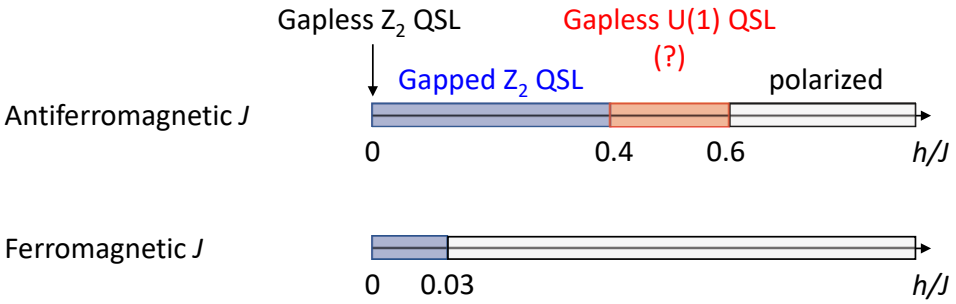

Fig. 6: *Schematic phase diagram of the isotropic Kitaev honeycomb model in a magnetic field along [111], i.e., with $h_x = h_y = h_z$. For antiferromagnetic coupling (top) the $\mathbb{Z}_2$ spin liquid is rather robust, and an intermediate second QSL emerges which is possibly of U(1) character. In contrast, for ferromagnetic coupling (bottom) a small field destroys the $\mathbb{Z}_2$ spin liquid in favor of a polarized phase [74].*

phases have been argued to be of first order [76]. Generally, liquid–VBS transitions may be realized in Heisenberg models with further-neighbor (e.g. J_1-J_2-J_3) exchange interactions. Instead of condensing visons one can consider condensing spinons in SU(2)-symmetric $\mathbb{Z}_2$ spin liquids. This produces a confined antiferromagnet with spiral order via an O(4)* transition [75, 78, 79] where the symmetry arises from a doublet of complex spinon fields. A resulting "global" phase diagram is shown in Fig. 7. Finally, condensing bound states of spinons and visons may induce conventional two-sublattice Néel order. At the latter transition, which is of more exotic type, both magnetic and VBS correlation functions acquire critical power laws [79]. In the absence of SU(2) symmetry, quantum numbers need to be reconsidered, but the general picture remains valid. One example here is the 2D toric-code model perturbed by an Ising interaction which has been shown to display a continuous transition of Ising* type from a $\mathbb{Z}_2$ liquid to a ferromagnetic phase driven by defect condensation [80]. A second example is the transition between a $\mathbb{Z}_2$ spin liquid and a superfluid phase in a Kagome-lattice XY model. This transition is in the XY* universality class and has been studied numerically in some detail in Ref. [81].

A transition in group (iii) is realized upon condensing objects which do *not* carry gauge charge, then leading to the coexistence of symmetry-breaking order and fractionalization. Hence, the transition involves the onset of symmetry breaking on the background of a fractionalized topological state – this has also been dubbed fractionalized quantum criticality. For instance, condensing a gauge-neutral Néel vector in a spin liquid yields an AF* phase, and a spin-Peierls instability of a spin liquid can result in a VBS* state. A nice example of the former has been proposed to occur in certain Kitaev-based spin-orbital liquids [82], while an example of the latter is the instability of Majorana Fermi surfaces in 3D Kitaev-based spin liquids [83].

Transitions between different spin-liquid phases, group (iv), have also been considered on the level of effective field theories. Ref. [84] has developed a theory for transitions between chiral and $\mathbb{Z}_2$ spin liquids in two space dimensions; such transitions have been argued to be equivalent to the condensation of an XY field coupled to a U(1) gauge field, where the critical XY field represents a singlet combination of spinons. A second case is the transition from a U(1) to a

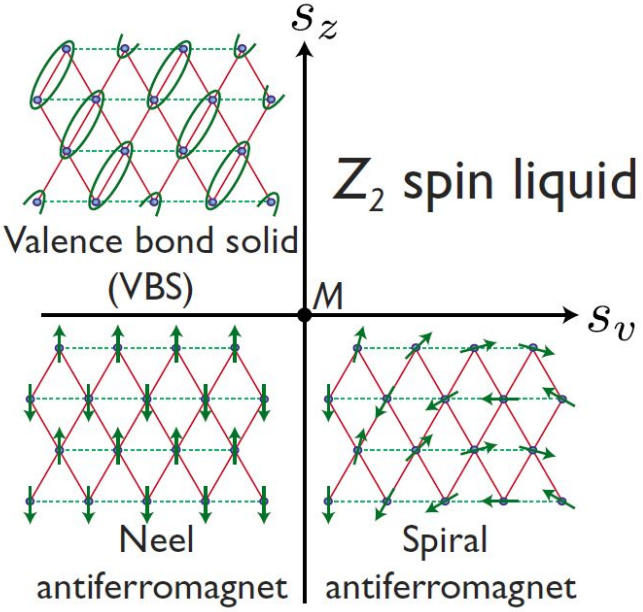

Fig. 7: *Global phase diagram for a 2D model of spinons with emergent $\mathbb{Z}_2$ gauge field, here shown for an anisotropic triangular lattice. The two parameters s_v and s_z represent masses of visons and spinons, respectively, in the doubled Chern-Simons theory considered in Ref. [75]. The spiral–$\mathbb{Z}_2$ spin liquid transition is described by a three-dimensional O(4)* theory, while the transition from VBS to $\mathbb{Z}_2$ spin liquid is of XY* type, see text. Further, the Néel–VBS transition is captured by a CP^1 theory (see Sec. 6.2 below), and the Néel–spiral transition is mean-field-like. (Figure taken from Ref. [75])*

$\mathbb{Z}_2$ spin liquid which is driven by the condensation of *pairs* of gauge-charged particles, akin to superconducting pairing. Such a transition has in fact been suggested to occur in the antiferromagnetic honeycomb Kitaev model in an applied magnetic field, Fig. 6: The small-field gapped $\mathbb{Z}_2$ spin liquid transits into a different spin liquid, suggested to be gapless and of U(1) type, before reaching the high-field phase [74, 85].

Among the few experimental examples of spin-liquid-related QPTs are field-driven transitions in suitable candidate materials, most notably in α-$RuCl_3$ and $NaYbX_2$ (X = S, Se, O). In α-$RuCl_3$ an intermediate-field spin liquid has been suggested to transit into the asymptotic high-field phase, with the transition being of first order [86]. In $NaYbX_2$, the zero-field spin liquid gives way to field-induced ordered states, but the nature of the quantum transition has not been probed in detail [34].

6.2 Deconfined quantum criticality

An interesting scenario for unconventional transitions between symmetry-broken states is that of deconfined quantum criticality [87]. It describes the possibility of a direct generic continuous QPT between two ordered states which break different symmetries. According to Landau theory and without fine-tuning, such a transition is forbidden, as it would be either of first order or split into two continuous transitions. At a deconfined quantum critical point, the critical degrees of

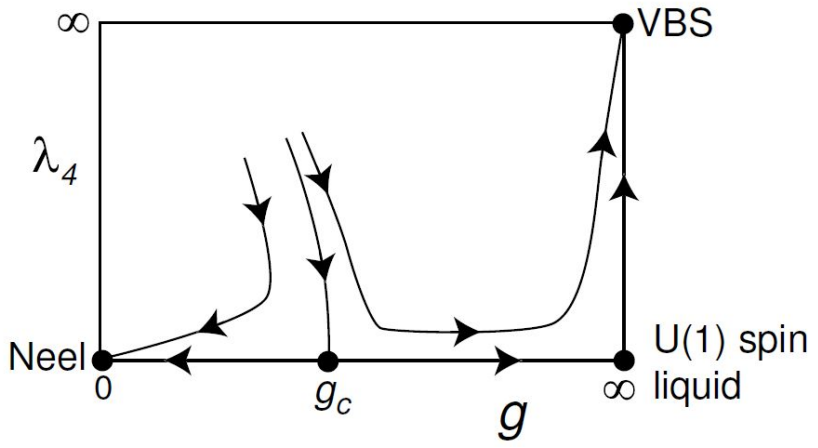

Fig. 8: *Schematic renormalization group flow proposed for the transition between a Néel antiferromagnet and a VBS in an SU(2)-symmetric magnet, as realized e.g., by the square-lattice spin-*$1/2$ *J-Q model. Increasing g destabilizes magnetic order; the parameter λ_4 represents the fugacity of monopoles in the U(1) gauge field. The horizontal axis $\lambda_4 = 0$ corresponds to the non-compact CP^1 theory of Eq.* (7)*, with g to be identified with the spinon mass s. (Figure taken from Ref. [89])*

freedom are fractionalized particles, and the order parameters of both phases are composites of these particles. This automatically leads to large anomalous exponents for order-parameter correlations.

The most thoroughly studied instance of deconfined quantum criticality is the transition between a Néel-ordered antiferromagnet and a valence-bond solid on the square lattice. The proposed field theory employs a CP^1 representation of spins, with deconfined bosonic spinons z_α and a U(1) gauge field A_μ, resulting in the action

$$\mathcal{S} = \int d^d x d\tau \left[\left| (\partial_\mu - i A_\mu) z_\alpha \right|^2 + s |z_\alpha|^2 + \frac{u}{2} \left(|z_\alpha|^2 \right)^2 + \frac{1}{2e^2} \left(\epsilon_{\mu\nu\lambda} \partial_\nu A_\lambda \right)^2 \right] \tag{7}$$

with the last term encoding the gauge-field dynamics. The primary transition, accessed by the variation of the mass parameter s, is that between a U(1) spin liquid and a Néel antiferromagnet. It is driven by the condensation of the z spinons which induces confinement via a Higgs mechanism; at this transition the gauge field can be assumed to be non-compact, as in the continuum limit of Eq. (7). However, the U(1) gauge field microscopically emerges from a complex-phase degree of freedom of the spinons and is therefore compact. This implies the existence of monopoles, and their condensation renders the U(1) spin liquid unstable towards a dimerized confined VBS phase, Fig. 8. Hence, deconfined spinons exist only at criticality [87–89].

The above proposal has been tested in detailed numerical simulations of the so-called J-Q model on the square lattice, where Q denotes the strength of a ring-exchange term [90]. While these simulations have verified a large part of the phenomenology of deconfined quantum criticality [90, 91], they have also found evidence for large logarithmic corrections to scaling which are not predicted by the field-theoretical framework [92]. We also note that direct numerical simulations of the proposed CP^1 field theory have found indications for the transition being weakly first order [93], a tendency which could not be confirmed in the J-Q model simulations.

The reasons for these discrepancies in numerical results are open, see Ref. [94] for a discussion.

Recent developments in the context of field-theoretical dualities have led to additional insights [95]. It has been conjectured that the non-compact CP^1 model is dual to a so-called QED_3 Gross-Neveu model at criticality, the latter describing Dirac fermions coupled to both a U(1) gauge field and local Ising degrees of freedom. This duality suggests that the deconfined QCP between a Néel antiferromagnet and a VBS displays an emergent SO(5) symmetry, which is supported by numerical results [94]. A weak first-order transition with quasi-universal behavior in its vicinity appears as a plausible scenario [96].

In addition to the Néel-VBS transition, various other Landau-forbidden transitions between two differently ordered phases have been discussed in the context of deconfined criticality. For instance, the transitions between a $\mathbb{Z}_2$ spin liquid and a VBS discussed in Sec. 6.1, as well as a transition between a $\mathbb{Z}_2$ spin liquid and a Néel state, also belong to this class, as a $\mathbb{Z}_2$ spin liquid displays topological order. Emergent higher symmetries, which can be rationalized via suitable dualities, appear to be common to many of the deconfined critical points [95].

Although a clear-cut experimental example realizing deconfined quantum criticality is lacking, a recently identified candidate is the frustrated Shastry-Sutherland magnet $SrCu_2(BO_3)_2$. Under applied pressure, it displays a transition from a plaquette VBS to an antiferromagnetic phase [97] which has been argued to be a deconfined QPT [98].

7 Mott and Kondo transitions

While all material presented so far was devoted to Mott insulators with local moments, we now turn to QPTs involving metallic phases [4]. For metals, the concepts of symmetry breaking and local order parameters apply equally, hence symmetry-breaking QPTs can be defined and characterized in analogy to insulators. However, the presence of low-energy particle–hole excitations and their coupling to order-parameter fluctuations complicates the theoretical analysis: Following the spirit of LGW theory requires to integrate out the particle–hole excitations to arrive at a theory for the order parameter alone; this approach has been developed in detail in the works of Hertz [2], Millis [99], and Moriya [100]. However, it was later realized that such an LGW theory is plagued with singularities. Consequently, more refined approaches keeping both order-parameter and fermionic fluctuations are required, and some progress has been made [101–104].

In this section, we will exclusively deal with even more intricate types of QPT, namely those involving the onset or loss of metallicity. Historically, the interaction-driven Mott transition has been discussed extensively. A younger topic is that of partial Mott transitions in multi-band or multi-orbital systems, with a subclass being transition where the Kondo effect breaks down. We will discuss these transitions – together with their relation to frustration – below.

7.1 Fermi liquids and non-Fermi liquids

Before diving into the physics of Mott transitions, we need to review some aspects of the low-energy physics of metals. The key concept is that of a Fermi liquid, which asserts a one-to-one correspondence of the low-energy many-body states between the interacting system under consideration and a hypothetical system of non-interacting electrons. This implies in particular the existence of quasiparticle excitations with charge $\pm e$ and spin $1/2$ (and forbids the existence of other low-energy excitations!). It also implies the existence of a Fermi surface, defined by the location of jumps in the momentum distribution $\langle n_{k\sigma}\rangle$ (or, equivalently, poles of the single-particle spectral function at $\omega = 0$). This Fermi surface then obeys Luttinger's theorem, i.e., has a momentum-space volume given by the total density of electrons n_{tot} (modulo filled bands):

$$\mathcal{V}_{\text{FL}} = K_d(n_{\text{tot}} \bmod 2) \tag{8}$$

where factors of 2 account for spin degeneracy, i.e., a full band corresponds to $n = 2$, and $K_d = (2\pi)^d/(2V_0)$ where V_0 is the unit-cell volume [105]. Under these conditions, the standard low-temperature Fermi-liquid properties $C(T) = \gamma T,\ \rho(T) = \rho_0 + AT^2$ etc., with γ, A being constants, follow immediately.[5]

Violations of Fermi-liquid behavior at low temperature, generically dubbed non-Fermi liquid, can have various sources. In clean systems, interaction effects can produce stable non-Fermi-liquid phases. One scenario is that the low-energy excitations display quantum numbers different that of from electron or holes, leading to distinct low-temperature properties. While such behavior is generic and well understood in $d = 1$, resulting in Luttinger liquids with spin-charge separation, similarly controlled descriptions in higher dimensions are scarce. A viable route to spin-charge-fractionalized metals is the doping of spin liquids [106].

Another scenario for stable non-Fermi liquids in $d \geq 2$ has been termed fractionalized Fermi liquid [107, 108]. In such a phase, charged excitations have conventional quantum numbers (charge $\pm e$ and spin $1/2$), but these coexist with additional deconfined fractionalized degrees of freedom. A generic construction starts from a fractionalized spin liquid and adds conventional carriers in a second band. If these subsystems remain weakly coupled, they realize a FL* phase (which has also been characterized as metallic spin liquid in the literature). Importantly, such a phase displays a Fermi surface with a volume violating Luttinger's theorem (8) in a quantized fashion, often [107]

$$\mathcal{V}_{\text{FL}^*} = K_d((n_{\text{tot}}-1) \bmod 2) \tag{9}$$

where the -1 accounts for the electrons forming the spin-liquid component. Low-temperature properties may or may not be Fermi-liquid-like, depending on whether the emergent excitations of the spin-liquid component are gapped or gapless. Fractionalized Fermi liquids may display a variety of instabilities driven by the strong correlations in the local-moment sector, including unconventional superconductivity [107, 109].

[5] A T^2 behavior of the resistivity requires the existence of Umklapp scattering processes, i.e., a sufficiently large Fermi surface.

Importantly, fractionalized Fermi liquids as well as other doped spin liquids are symmetric states (i.e. without spontaneously broken symmetries) with fractionalized excitations, much like insulating spin liquids. Given the insights into topological properties of fractionalized insulating phases, one may wonder about the topological characterization of non-Fermi-liquid metals. To our knowledge, relatively little work has been done in this direction. A sharp distinction between FL and FL* is the Fermi volume, and this can be considered a topological distinction. In contrast, some of the indicators established for insulators, like ground-state degeneracies and entanglement, cannot be easily applied because of the absence of an excitation gap [109], and more work is needed to clarify the topological nature of non-Fermi liquid metals.

7.2 Mott transitions

A Mott transition is an interaction-driven metal-to-insulator transition: It transforms a half-filled metallic band into an insulator of local moments. The most generic Hamiltonian for this physics is the Hubbard model of spinful electrons

$$\mathcal{H} = -t \sum_{\langle ij \rangle \sigma} \left(c^\dagger_{i\sigma} c_{j\sigma} + h.c. \right) + U \sum_i n_{i\uparrow} n_{i\downarrow} \tag{10}$$

where the Mott insulator occurs for $U \gg t$. The Mott-insulating state is often accompanied by antiferromagnetic long-range order, and the quantum transition from a paramagnetic metal to an antiferromagnetic Mott insulator is generically of first order (or involves an intermediate antiferromagnetic metallic phase). This is different in the case of a spin-liquid Mott insulator: A "genuine" zero-temperature Mott transition from a paramagnetic metal to an insulating spin liquid can be continuous. As the existence of the spin liquid requires frustration, such transitions are expected to occur in half-filled Hubbard models on frustrated lattices upon varying U/t. In fact, a metal-to-spin liquid transition has been found in numerical simulations of the triangular-lattice Hubbard model which, however, appears to be first order [110, 111], Fig. 9, with superconductivity possibly appearing on the metallic side before the Mott transition [111]. A candidate experimental realization is in the organic compound κ-$(ET)_2Cu_2(CN)_3$ under pressure [112].

A defining criterion for a Mott transition is a quantized change in the Fermi volume: In a Fermi liquid, the momentum-space volume enclosed by the Fermi surface is given by the total number of electrons according to Luttinger's theorem (8). In a Mott insulator, there is no Fermi surface[6], and hence the Fermi volume changes at a single-band Mott transition by $K_d \times 1$. Such an abrupt change is nevertheless compatible with the QPT being continuous: Upon approaching a continuous Mott transition from the metallic side, the quasiparticle weight on the Fermi surface will vanish continuously, while the charge gap opens continuously on the insulating side. At criticality, one expects a *critical Fermi surface*, i.e., a well-defined $(d-1)$-dimensional mani-

[6] We do not consider the so-called Luttinger volume, $V_{\rm lutt} = \int_{G(k)>0} dk$, which accounts for both poles and zeroes of the Green's function. For an in-depth discussion on aspects of the Luttinger volume in Mott insulators see Ref. [113].

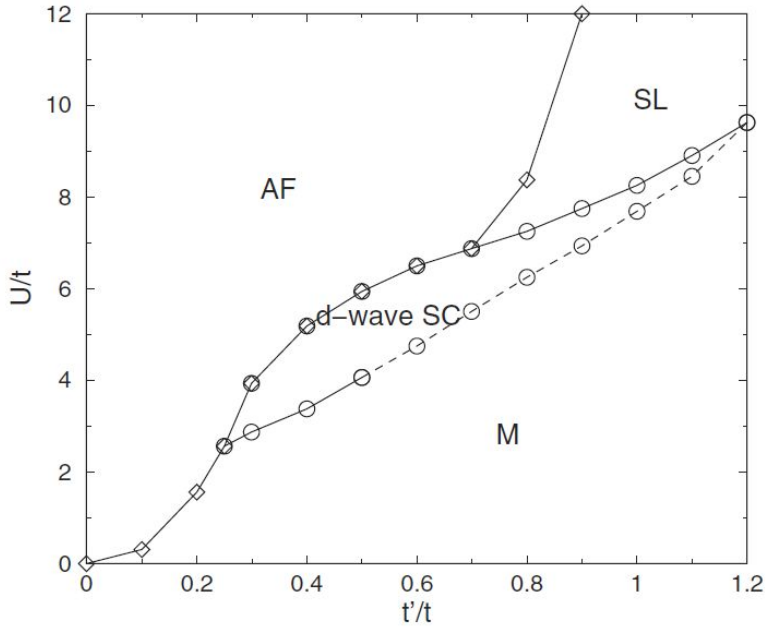

Fig. 9: *Cluster-DMFT phase diagram of the Hubbard model on an anisotropic triangular lattice as function of Hubbard interaction U and hopping ratio t'/t, where $t' = 0$ and $t' = t$ correspond to the square and triangular lattices, respectively. M, SC, AF, SL denote metal, superconductor, antiferromagnetic insulator, and spin-liquid phases, respectively. Solid (dashed) lines correspond to first-order (continuous) transitions. (Figure taken from Ref. [111])*

fold in momentum space where the electronic spectral function displays (possibly momentum dependent) power-law singularities [114].

A concise theoretical understanding of continuous zero-temperature Mott transitions is lacking to date. Most theoretical descriptions are based on slave-particle theories which involve separate degrees of freedom representing spin and charge of the electrons. Often, the charge degrees of freedom are encoded by bosons which are gapless and condensed in the metal, but gapped and disordered in the insulator. Hence, the insulator-to-metal transition becomes a BEC transition of charged bosons coupled to a gauge field [115]. However, such a description (at least in its simplest version) does not account for possible non-trivial momentum dependencies along the Fermi surface. Moreover, the fermionic character of the Mott phenomenon might require a formulation using non-bosonic critical degrees of freedom, but to our knowledge a successful theory of this type has not been formulated.

It is worth noting that apparent quantum critical behavior at elevated temperatures has been detected above the finite-temperature endpoint of a first-order Mott transition line. This remarkable observation, manifest, e.g., in scaling behavior of the resistivity, was first made in DMFT simulations of the single-band Hubbard model on a Bethe lattice [116], and later verified experimentally in three pressure-tuned organic compounds [117]. Subsequent work has linked this behavior to a $T = 0$ scale-invariant quantum critical insulator at the boundary of the metal–insulator phase coexistence regime [118].

7.3 Kondo and orbital-selective Mott transitions

In a multi-band or multi-orbital system, there is the possibility for a partial Mott transition. This is a transition between two *metallic* phases where the Fermi surface undergoes a quantized change. In the simplest case, one band (or orbital) changes its character from metallic to Mott-insulating while other bands remain metallic. Consequently, such a transition has also been dubbed orbital-selective Mott transition [119–121]. If stable in the low-temperature limit, the partial Mott phase violates Luttinger's theorem (8) and, hence, is a non-Fermi liquid metal. This is precisely the fractionalized Fermi-liquid phase (FL*) introduced in Sec. 7.1 above, and a transition between FL and FL* is an orbital-selective Mott transition (or a deconfinement transition in the language of the underlying gauge theory). Phenomenologically, such a transition can be expected to be accompanied by a jump in the Hall constant [122].

A natural territory for orbital-selective Mott physics are heavy-fermion metals [4, 123], as described by the Kondo-lattice Hamiltonian

$$\mathcal{H} = -t \sum_{\langle ij\rangle\sigma} \left(c^\dagger_{i\sigma} c_{j\sigma} + h.c. \right) + J \sum_i \vec{S}_i \cdot \vec{s}_i, \tag{11}$$

with J the Kondo coupling and $\vec{s}_i = \sum_{\sigma\sigma'} c^\dagger_{i\sigma} \vec{\tau}_{\sigma\sigma'} c_{i\sigma'}/2$ the conduction-electron spin density on site i. As pointed out early on by Doniach [124], the heavy-fermion phase diagram is governed by the competition between Kondo screening and RKKY interactions between local moments, leading to heavy Fermi liquids and ordered magnetic states, respectively. Later on, it has been suggested [108, 125–127] to consider, in addition to the ratio between Kondo temperature and RKKY interaction, a second tuning parameter which acts to suppress magnetic order in the local-moment subsystem – this is loosely labelled as "frustration" (alternatively: "quantum fluctuations"). This tuning parameter naturally enables access to fractionalized states. If RKKY interactions are sufficiently frustrated, then increasing them w.r.t. the Kondo scale leads to a breakdown of the Kondo effect without concomitant magnetic order, generically resulting in an FL* phase.

The resulting "global" phase diagram of heavy fermions is shown in Fig. 10. It features two transition lines, one involving the onset of antiferromagnetism and one involving the onset of deconfinement. Importantly, the onset of deconfinement in the paramagnetic metallic phase corresponds to an orbital-selective Mott transition into an FL* phase as advocated above, as FL* features deconfined fractionalized excitations in the local-moment sector. Such an orbital-selective Mott transition is easily driven by the reduction of Kondo screening in a frustrated regime, because it is Kondo screening which renders the local-moment electrons metallic. Hence, the onset of deconfinement also corresponds to a breakdown of the Kondo effect. The two transition lines define four phases: In addition to the paramagnetic phases FL and FL*, there are a conventional (AF) and a fractionalized (AF*) antiferromagnet. The Fermi volume is "large" in the FL phase, i.e., encloses both conduction and local-moment electrons, while it is "small" in FL* because it is determined by conduction electrons alone, hence violating Luttinger's theorem. In the metallic AF and AF* phase, translation symmetry breaking enlarges the unit cell,

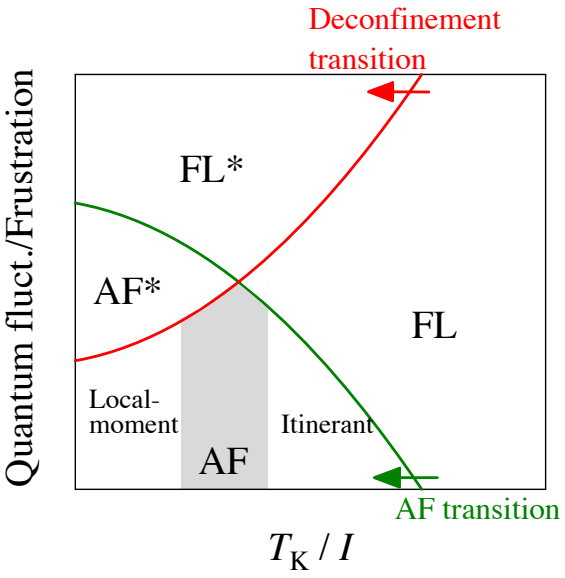

Fig. 10: *"Global" phase diagram for heavy-fermion metals (with one f electron per crystallographic unit cell), with two transitions for the onset of antiferromagnetism and for the breakdown of the Kondo effect (equivalently the onset of deconfinement). FL* is the fractionalized Fermi-liquid phase described in Sec. 7.1. Inside the AF phase, a crossover from more itinerant to more localized behavior occurs, which may be accompanied by one or more transitions where the Fermi-surface topology changes. Lastly, AF* refers to a fractionalized magnet, with magnetic LRO and fractionalized excitations coexisting. (Figure taken from Ref. [127])*

such that Luttinger's theorem is generically fulfilled. The transition from FL to AF is hence a conventional ordering transition, accompanied by the backfolding of bands.
A slightly different version of the global phase diagram has been put forward in Ref. [125], the main difference being that the coincidence of the Kondo-breakdown and magnetic transition lines is not considered accidental, but systematic. Ref. [128] has developed a corresponding extended DMFT description of a Kondo breakdown driven by magnetic criticality. Alternatively, this might be viewed as a case of deconfined criticality [129].

8 Summary

Frustrated magnetism and quantum criticality both constitute highly active fields of research in condensed matter physics, and both have received additional fuel in the last two decades by the improved understanding of topological phenomena in solids. This chapter aimed at an overview of the interplay of both, frustration and quantum criticality, with focus on theoretical ideas and concepts as well as links to current experiments in correlated-electron materials. While quantum criticality in clean insulators is mainly well understood, frustration brings in new ingredients – large degeneracies, order by disorder, and fractionalization – which often change the rules of the game, and we have discussed a few particularly fascinating outcomes. In metallic systems, the physics of quantum phase transitions is more complicated in general, due to the presence of low-energy fermions, with many open questions even without frustration. Clearly, this fascinating field invites more work, both theoretical and experimental.

References

[1] This chapter heavily draws from the review articles [5] and [6].

[2] J.A. Hertz, Phys. Rev. B **14**, 1165 (1976)

[3] S. Sachdev: *Quantum Phase Transitions*, 2nd ed. (Cambridge University Press, 2010)

[4] H. von Löhneysen, A. Rosch, M. Vojta, and P. Wölfle, Rev. Mod. Phys. **79**, 1015 (2007)

[5] M. Vojta, Rep. Prog. Phys. **81**, 064501 (2018)

[6] M. Vojta, Rep. Prog. Phys. **66**, 2069 (2003)

[7] C. Rüegg *et al.*, Nature **423**, 62 (2003); Phys. Rev. Lett. **93**, 257201 (2004)

[8] A.P. Ramirez, Ann. Rev. Mat. Sci. **24**, 453 (1994)

[9] L. Balents, Nature **464**, 199 (2010)

[10] O.A. Starykh, Rep. Prog. Phys. **78**, 052502 (2015)

[11] L. Savary and L. Balents, Rep. Prog. Phys. **80**, 016502 (2017)

[12] Y. Zhou, K. Kanoda, and T.-K. Ng, Rev. Mod. Phys. **89**, 025003 (2017)

[13] C. Lacroix, P. Mendels, and F. Mila (Eds.): *Introduction to Frustrated Magnetism* (Springer, Heidelberg, 2011)

[14] A. Kitaev, Ann. Phys. (N.Y.) **321**, 2 (2006)

[15] S.T. Bramwell and M.J.P. Gingras, Science **294**, 1495 (2001)

[16] G.H. Wannier, Phys. Rev. **79**, 357 (1950)

[17] L. Pauling, J. Am. Chem. Soc. **57**, 2680 (1935)

[18] C. Castelnovo, R. Moessner, and S. L Sondhi, Nature **451**, 42 (2008)

[19] A. Kitaev and J. Preskill, Phys. Rev. Lett. **96**, 110404 (2006)

[20] M. Levin and X.-G. Wen, Phys. Rev. Lett. **96**, 110405 (2006)

[21] X.G. Wen, Phys. Rev. B **65**, 165113 (2002)

[22] E.H. Lieb, T.D. Schultz, and D.C. Mattis, Ann. Phys. (N.Y.) **16**, 407 (1961)

[23] M.B. Hastings, Phys. Rev. B **69**, 104431 (2004)

[24] P.W. Anderson, Mater. Res. Bull. **8**, 153 (1973)

[25] R. Moessner and S.L. Sondhi, Phys. Rev. Lett. **86**, 1881 (2001)

[26] S. Yan, D.A. Huse, and S.R. White, Science **332**, 1173 (2011)

[27] Y. Iqbal, F. Becca, S. Sorella, and D. Poilblanc, Phys. Rev. B **87**, 060405(R) (2013)

[28] Y.-C. He, M.P. Zaletel, M. Oshikawa, and F. Pollmann, Phys. Rev. X **7**, 031020 (2017)

[29] J.S. Helton *et al.*, Phys. Rev. Lett. **98**, 107204 (2007)

[30] M.R. Norman, Rev. Mod. Phys. **88**, 041002 (2016)

[31] H.-C. Jiang, H. Yao, and L. Balents, Phys. Rev. B **86**, 024424 (2012)

[32] Z. Zhu and S.R. White, Phys. Rev. B **92**, 041105(R) (2015)

[33] M. Baenitz *et al.*, Phys. Rev. B **98**, 220409(R) (2018)

[34] M.M. Bordelon *et al.*, Nat. Phys. **15**, 1058 (2019)

[35] J. Villain, R. Bidaux, J.-P. Carton, and R. Conte, J. Phys. France **41**, 1263 (1980)

[36] M.E. Zhitomirsky, M.V. Gvozdikova, P.C.W. Holdsworth, and R. Moessner, Phys. Rev. Lett. **109**, 077204 (2012)

[37] U.K. Rößler, A.N. Bogdanov, and C. Pfleiderer, Nature **442**, 797 (2006)

[38] M. Blume and Y. Hsieh, J. Appl. Phys. **40**, 1249 (1969)

[39] H. Chen and P. Levy, Phys. Rev. Lett. **27**, 1383 (1971)

[40] A. Läuchli, F. Mila, and K. Penc, Phys. Rev. Lett. **97**, 087205 (2006); *ibid.* **97**, 229901 (2006)

[41] K. O'Brien, M. Hermanns, and S. Trebst, Phys. Rev. B **93**, 085101 (2016)

[42] K.W. Plumb *et al.*, Phys. Rev. B **90**, 041112 (2014)

[43] A. Banerjee *et al.*, Science **356**, 1055 (2017)

[44] Y. Singh and P. Gegenwart, Phys. Rev. B **82**, 064412 (2010)

[45] S.H. Chun *et al.*, Nat. Phys. **11**, 462 (2015)

[46] Y. Singh, S. Manni, J. Reuther, T. Berlijn, R. Thomale, W. Ku, S. Trebst, and P. Gegenwart, Phys. Rev. Lett. **108**, 127203 (2012)

[47] T. Takayama *et al.*, Phys. Rev. Lett. **114**, 077202 (2015)

[48] K.A. Modic *et al.*, Nat. Commun. **5**, 4203 (2018)

[49] K.I. Kugel and D.I. Khomskii, Sov. Phys. Usp. **25**, 231 (1982)

[50] G. Khaliullin and S. Maekawa, Phys. Rev. Lett. **85**, 3950 (2000)

[51] H. Yao and D.-H. Lee, Phys. Rev. Lett. **107**, 087205 (2011)

[52] H. Kawamura, J. Phys. Soc. Jpn. **54**, 3220 (1985); **56**, 474(1987);
Phys. Rev. B **38**, 4916 (1988)

[53] M. Tissier, B. Delamotte, and D. Mouhanna, Phys. Rev. Lett. **84**, 5208 (2000)

[54] S. Mühlbauer *et al.*, Science **323**, 915 (2009)

[55] C. Pfleiderer, P. Böni, T. Keller, U.K. Rössler, and A. Rosch, Science **316**, 1871 (2007)

[56] J.V. José, L.P. Kadanoff, S. Kirkpatrick, and D.R. Nelson, Phys. Rev. B **16**, 1217 (1977)

[57] J. Chaloupka, G. Jackeli, and G. Khaliullin, Phys. Rev. Lett. **105**, 027204 (2010)

[58] C.C. Price and N.B. Perkins, Phys. Rev. B **88**, 024410 (2013)

[59] R. Schaffer, S. Bhattacharjee, and Y.-B. Kim, Phys. Rev. B **86**, 224417 (2012)

[60] J. Chaloupka, G. Jackeli, and G. Khaliullin, Phys. Rev. Lett. **110**, 097204 (2013)

[61] M. Gohlke, R. Verresen, R. Moessner, and F. Pollmann,
Phys. Rev. Lett. **119**, 157203 (2017)

[62] M. Garst, L. Fritz, A. Rosch, and M. Vojta, Phys. Rev. B **78**, 235118 (2008)

[63] T. Giamarchi, C. Rüegg, and O. Tchernyshyov, Nat. Phys. **4**, 198 (2008)

[64] N. Laflorencie and F. Mila, Phys. Rev. Lett. **99**, 027202 (2007)

[65] Y.H. Matsuda *et al.*, Phys. Rev. Lett. **111**, 137204 (2013)

[66] V. Tsurkan *et al.*, Sci. Adv. **3**, e1601982 (2017)

[67] N. Shannon, T. Momoi, and P. Sindzingre, Phys. Rev. Lett. **96**, 027213 (2006)

[68] L. Janssen, E.C. Andrade, and M. Vojta, Phys. Rev. B **96**, 064430 (2017)

[69] F.A. Bais and J.K. Slingerland, Phys. Rev. B **79**, 045316 (2009)

[70] A.Y. Kitaev, Ann. Phys. (N.Y.) **303**, 2 (2003)

[71] J. Vidal, S. Dusuel, and K.P. Schmidt, Phys. Rev. B **79**, 033109 (2009)

[72] M. Schuler, S. Whitsitt, L.-P. Henry, S. Sachdev, and A.M. Läuchli,
Phys. Rev. Lett. **117**, 210401 (2016)

[73] H.-C. Jiang, Z.-C. Gu, X.-L. Qi, and S. Trebst, Phys. Rev. B **83**, 245104 (2011)

[74] C. Hickey and S. Trebst, Nat. Commun. **10**, 530 (2019)

[75] C. Xu and S. Sachdev, Phys. Rev. B **79**, 064405 (2009)

[76] C. Xu and L. Balents, Phys. Rev. B **84**, 014402 (2011)

[77] K. Slagle and C. Xu, Phys. Rev. B **89**, 104418 (2014)

[78] A.V. Chubukov, T. Senthil, and S. Sachdev, Phys. Rev. Lett. **72**, 2089 (1994); A.V. Chubukov, S. Sachdev, and T. Senthil, Nucl. Phys. B **426**, 601 (1994)

[79] E.-G. Moon and C. Xu, Phys. Rev. B **86**, 214414 (2012)

[80] Y. Kamiya, Y. Kato, J. Nasu, and Y. Motome, Phys. Rev. B **92**, 100403(R) (2015); Phys. Rev. B **93**, 179902 (2016)

[81] S.V. Isakov, R.G. Melko, and M.B. Hastings, Science **335**, 193 (2012)

[82] U.F.P. Seifert, X.-Y. Dong, S. Chulliparambil, M. Vojta, H.-H. Tu, and L. Janssen, Phys. Rev. Lett. **125**, 257202 (2020)

[83] M. Hermanns, S. Trebst, and A. Rosch, Phys. Rev. Lett. **115**, 177205.

[84] M. Barkeshli, arXiv:1307.8194.

[85] N.D. Patel and N. Trivedi, PNAS **116**, 12199 (2019)

[86] S. Suetsugu *et al.*, J. Phys. Soc. Jpn. **91**, 124703 (2022)

[87] T. Senthil, A. Vishwanath, L. Balents, S. Sachdev, and M.P.A. Fisher, Science **303**, 1490 (2004)

[88] T. Senthil, L. Balents, S. Sachdev, A. Vishwanath, and M.P.A. Fisher, Phys. Rev. B **70**, 144407 (2004)

[89] T. Senthil, L. Balents, S. Sachdev, A. Vishwanath, and M.P.A. Fisher, J. Phys. Soc. Jpn. **74** Suppl. 1 (2005)

[90] A. Sandvik, Phys. Rev. Lett. **98**, 227202 (2007)

[91] R.G. Melko and R.K. Kaul, Phys. Rev. Lett. **100**, 017203 (2008)

[92] A. Sandvik, Phys. Rev. Lett. **104**, 177201 (2010)

[93] A.B. Kuklov, M. Matsumoto, N.V. Prokof'ev, B.V. Svistunov, and M. Troyer, Phys. Rev. Lett. **101**, 050405 (2008)

[94] A. Nahum, J.T. Chalker, P. Serna, M. Ortuno, and A.M. Somoza, Phys. Rev. X **5**, 041048 (2015)

[95] C. Wang, A. Nahum, M.A. Metlitski, C. Xu, and T. Senthil, Phys. Rev. X **7**, 031051 (2017)

[96] A. Nahum, Phys. Rev. B **102**, 201116(R) (2020)

[97] M.E. Zayed *et al.*, Nat. Phys. **13**, 962 (2017)

[98] J.Y. Lee, Y.-Z. You, S. Sachdev, and A. Vishwanath, Phys. Rev. X **9**, 041037 (2019)

[99] A.J. Millis, Phys. Rev. B **48**, 7183 (1993)

[100] T. Moriya: *Spin Fluctuations in Itinerant Electron Magnetism* (Springer, Berlin, 1985)

[101] S.-S. Lee, Phys. Rev. B **80**, 165102 (2009)

[102] M.A. Metlitski and S. Sachdev, Phys. Rev. B **82**, 075127 (2010); *ibid.* **82**, 075128 (2010)

[103] A. Schlief, P. Lunts, and S.-S. Lee, Phys. Rev. X **7**, 021010 (2017)

[104] M.H. Gerlach, Y. Schattner, E. Berg, and S. Trebst, Phys. Rev. B **95**, 035124 (2017)

[105] M. Oshikawa, Phys. Rev. Lett. **84**, 3370 (2000)

[106] P.A. Lee, N. Nagaosa, and X.-G. Wen, Rev. Mod. Phys. **78**, 17 (2006)

[107] T. Senthil, S. Sachdev, and M. Vojta, Phys. Rev. Lett. **90**, 216403 (2003)

[108] T. Senthil, M. Vojta, and S. Sachdev, Phys. Rev. B **69**, 035111 (2004)

[109] U.F.P. Seifert, T. Meng, and M. Vojta, Phys. Rev. B **97**, 085118 (2018)

[110] H. Morita, S. Watanabe, and M. Imada, J. Phys. Soc. Jpn. **71**, 2109 (2002)

[111] B. Kyung and A.M.S. Tremblay, Phys. Rev. Lett. **97**, 046402 (2006)

[112] Y. Shimizu, K. Miyagawa, K. Kanoda, M. Maesato, and G. Saito, Phys. Rev. Lett. **91**, 107001 (2003)

[113] A. Rosch, Eur. Phys. J. B **59**, 495 (2007)

[114] T. Senthil, Phys. Rev. B **78**, 035103 (2008)

[115] T. Senthil, Phys. Rev. B **78**, 045109 (2008)

[116] H. Terletska, J. Vucicevic, D. Tanasković, and V. Dobrosavljević, Phys. Rev. Lett. **107**, 026401 (2011)

[117] T. Furukawa, K. Miyagawa, H. Taniguchi, R. Kato, and K. Kanoda, Nat. Phys. **11**, 221 (2015)

[118] H. Eisenlohr, S.-S.B. Lee, and M. Vojta, Phys. Rev. B **100**, 155152 (2019)

[119] V. Anisimov, I. Nekrasov, D. Kondakov, T. Rice, and M. Sigrist, Eur. Phys. J. B **25**, 191 (2002)

[120] C. Pépin, Phys. Rev. Lett. **98**, 206401 (2007)

[121] M. Vojta, J. Low Temp. Phys. **161**, 203 (2010)

[122] P. Coleman, J.B. Marston, and A.J. Schofield, Phys. Rev. B **72**, 245111 (2005)

[123] P. Gegenwart, Q. Si, and F. Steglich, Nat. Phys. **4**, 186 (2008)

[124] S. Doniach, Physica B **91**, 231 (1977)

[125] Q. Si, Physica B **378-380**, 23 (2006); Phys. Stat. Sol. B **247**, 476 (2010)

[126] P. Coleman and A.H. Nevidomskyy, J. Low. Temp. Phys. **161**, 182 (2010)

[127] M. Vojta, Phys. Rev. B **78**, 125109 (2008)

[128] Q. Si, S. Rabello, K. Ingersent, and J.L. Smith, Nature **413**, 804 (2001); Phys. Rev. B **68**, 115103 (2003)

[129] T. Senthil, S. Sachdev, and M. Vojta, Physica B **359-361**, 9 (2005)